Inorganic Chemistry

ARTICLE

pubs.acs.org/IC

Crystal Structure and Physical Properties of the New Chalcogenides $Ba_3Cu_{17-x}(S,Te)_{11}$ and $Ba_3Cu_{17-x}(S,Te)_{11.5}$ with Two Different Cu Clusters

Bryan A. Kuropatwa, Abdeljalil Assoud, and Holger Kleinke*

Department of Chemistry, University of Waterloo, Waterloo, Ontario N2L 3G1, Canada

Supporting Information

ABSTRACT: The sulfide-tellurides $Ba_3Cu_{17-x}(S,Te)_{11}$ and $Ba_3Cu_{17-x}(S,Te)_{11.5}$ were synthesized from the elements in stoichiometric ratios heated to 1073 K, followed by slow cooling to 873 K over 100 h. $Ba_3Cu_{17-x}(S,Te)_{11}$ is isostructural to $Ba_3Cu_{17-x}(Se,Te)_{11}$ when [S] > [Te], space group $R\bar{3}m$, with lattice dimensions of a = 12.009(1) Å, c = 27.764(2) Å, V = 3467.6(5) Å^3, for $Ba_3Cu_{15.7(4)}S_{7.051(5)}Te_{3.949}$ (Z = 6). The structure is composed of Cu atoms forming paired hexagonal antiprisms, capped on the two outer hexagonal faces, where each Cu atom is tetrahedrally coordinated by four Q (= S, Te) atoms. The new variant is formed when [Te] > [S]; then $Ba_3Cu_{17-x}(S,Te)_{11.5}$ adopts space group $Fm\bar{3}m$ with a = 17.2095(8) Å, V = 5096.9(4) Å^3, for $Ba_3Cu_{15.6(2)}S_{5.33(4)}Te_{6.17}$ (Z = 8). This structure consists of eight Te-centered Cu_{16} icosioctahedra per cell interconnected by cubic Cu_8 units centered by Q atoms. Electronic structure calculations and property measurements illustrate that these compounds behave as extrinsic p-type semiconductors—toward metallic behavior for the latter compound. With standard oxidation states Ba^{2+}, Cu^+, and Q^{2-}, the electron precise formulas are $Ba_3Cu_{16}Q_{11}$ and $Ba_3Cu_{17}Q_{11.5}$.

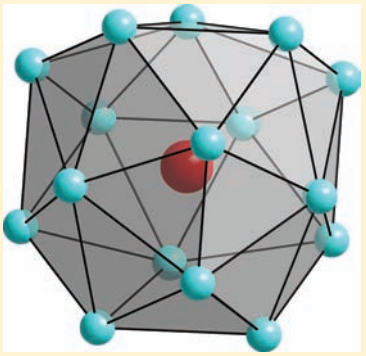

INTRODUCTION

The special bonding in polychalcogenides as in $HfTe_5$[1] and the phase-change material $Ag_{10}Te_4Br_3$[2] led us to investigate the systems Ba−Cu/Ag-Q with Q = S, Se, Te, following reports concerning thermoelectric properties[3−5] of $BaCu_2Te_2$[6] and $A_2BaCu_8Te_{10}$ (A = K, Rb, Cs).[7] Investigation into this family of compounds led to the discovery of several new ternary and quaternary compounds in this group, the first of which has the formula $Ba_3Cu_{14-x}Te_{12}$.[8] On further pursuit of this system, we uncovered higher chalcogenides such as $Ba_2Cu_{6-x}STe_4$ and $Ba_2Cu_{6-x}Se_yTe_{5-y}$,[9] $BaCu_{6-x}S_{1-y}Te_{6+y}$ and $BaCu_{6-x}Se_{1-y}Te_{6+y}$,[10] and $Ba_2Cu_{4-x}Se_yTe_{5-y}$,[11] in part with polychalcogenide groups. All of these structures only form when using two different chalcogen atoms (the ternary telluride $Ba_2Cu_{4-x}Te_5$ adopts a structure type different to $Ba_2Cu_{4-x}Se_yTe_{5-y}$).[11]

By again following the concept of *differential fractional site occupancy* (DFSO)[12,13] with respect to the anionic components[14,15]—the same approach that also led to the discovery of $Nb_{1.72}Ta_{3.28}S_2$,[16] $Nb_{0.95}Ta_{1.05}S$,[17] $Nb_{4.92}Ta_{6.08}S_4$,[18] and $Nb_{6.74}Ta_{5.26}S_4$[19] with fractional occupancies of the cations—we were able to discover another unique structure type in the plentiful Ba−Cu-Q system: $Ba_3Cu_{17-x}Q_{11}$[20] with $1 < x \leq 2.7$, Q = Se, Te. While replacing selenium by sulfur, we now revealed the existence of a new structure type, $Ba_3Cu_{17-x}Q_{11.5}$, not found in the selenide-telluride system that occurs when [S] < [Te] and a structure analogous to $Ba_3Cu_{17-x}Q_{11}$ when [Te] < [S]. These two different sulfide-tellurides are introduced with this article.

EXPERIMENTAL SECTION

Synthesis. All reactions commenced from the elements (Ba: 99%, pieces, Aldrich; Cu: 99.5%, powder −150 mesh; Alfa Aesar; S: 99.98%, powder, Aldrich; Te: 99.999%, ingot, Aldrich), with sample masses of approximately 600 mg. The elements were stored and handled in a glovebox filled with argon. Inside that box, the elements were placed into silica tubes, which were subsequently sealed under vacuum (10^{-3} mbar). The tubes were then heated in a resistance furnace at 1073 K for 6 h. Thereafter, the furnace was slowly cooled down to 873 K and left for a period of 100 h to allow for homogenization. Lastly, the furnace was switched off, prompting fast cooling.

The rhombohedral variant was first encountered in a similar reaction with the Ba/Cu/S/Te ratio of 1:4:2:1, and identified as $Ba_3Cu_{15.1(1)}S_{7.92(2)}Te_{3.08}$ via the single crystal structure determination described below. The cubic variant was discovered in a reaction with the Ba/Cu/S/Te ratio of 1:4:1:2, and subsequently identified as $Ba_3Cu_{16.0(1)}S_{4.45(4)}Te_{7.05}$. Since its formula contained Cu deficient sites and mixed S:Te occupancies, several reactions were carried out to analyze the phase range of $Ba_3Cu_{17-x}S_{11-y}Te_y$. This formula results hypothetically with x = 0, when all filled Wyckoff sites are fully occupied. Variations of S:Te were studied with x = 0 or 1.0, while varying y between 2 and 9. Holding a constant y = 4 allowed for an additional study where x = 0, 0.5, 1.0, 1.5, 2. All samples were analyzed by means of X-ray powder diffraction, utilizing the INEL diffractometer with Cu−Kα_1 radiation. Samples were found pure-phase for x = 0.5, 1, or 1.5 with $2 \leq y \leq 5$, producing the

Received: May 10, 2011
Published: July 20, 2011

Table 1. Crystallographic Data for $Ba_3Cu_{17-x}(S,Te)_{11}$ and $Ba_3Cu_{17-x}(S,Te)_{11.5}$

refined formula	$Ba_3Cu_{15.1(1)}S_{7.92(2)}Te_{3.08}$	$Ba_3Cu_{15.7(4)}S_{7.051(5)}Te_{3.949}$	$Ba_3Cu_{15.6(2)}S_{5.33(4)}Te_{6.17}$	$Ba_3Cu_{16.0(1)}S_{4.45(4)}Te_{7.05}$
formula weight [g/mol]	2018.13	2139.96	2362.97	2473.81
T of measurement [K]	298(2)	298(2)	296(2)	293(2)
λ [Å]	0.71073	0.71073	0.71073	0.71073
space group	$R\bar{3}m$	$R\bar{3}m$	$Fm\bar{3}m$	$Fm\bar{3}m$
a [Å]	11.9371(3)	12.009(1)	17.2095(8)	17.2364(4)
c [Å]	27.522(2)	27.764(2)		
V [Å^3]	3396.3(2)	3467.6(5)	5096.9(4)	5120.8(2)
Z	6	6	8	8
μ [mm^{-1}]	23.601	24.628	24.625	25.763
ρ_{calcd} [g/cm^3]	5.927	6.149	6.159	6.417
$R(F_o)$,[a] $R_w(F_o^2)$[b]	0.0579, 0.1045	0.0199, 0.0283	0.0277, 0.0737	0.0287, 0.0544

[a] $R(F_o) = \Sigma||F_o| - |F_c||/\Sigma|F_o|$. [b] $R_w(F_o^2) = [\Sigma w(F_o^2 - F_c^2)^2/\Sigma w(F_o^2)^2]^{1/2}$.

Table 2. Atomic Coordinates and Equivalent Isotropic Displacement Parameters of $Ba_3Cu_{15.7(4)}S_{7.051(5)}Te_{3.949}$, and Occupancy Factors of $Ba_3Cu_{15.7(4)}S_{7.051(5)}Te_{3.949}$ and $Ba_3Cu_{15.1(1)}S_{7.92(2)}Te_{3.08}$

atom	site	x	y	z	U_{eq}/Å^2	occ.[a]	occ.[b]
Ba	18 h	0.47016(1)	0.52984(1)	0.086879(9)	0.01327(7)	1	1
Cu1	36i	0.22846(5)	0.01116(4)	0.13437(2)	0.0246(2)	0.987(2)	0.915(7)
Cu2	18 h	0.4274(6)	0.5726(6)	0.3480(3)	0.027(3)	0.49(6)	0.94(1)
Cu2B[c]	36i	0.446(2)	0.610(2)	0.3507(3)	0.026(1)	0.24(3)	
Cu3	18 h	0.52308(3)	0.47692(3)	0.28218(2)	0.0221(2)	0.987(3)	1
Cu4	18 h	0.54696(3)	0.45304(3)	0.37877(2)	0.0233(2)	0.979(3)	0.96(1)
Cu5	6c	0	0	0.16634(4)	0.0217(4)	0.954(5)	0.78(2)
Cu6	6c	$^1/_3$	$^2/_3$	0.399(3)	0.02(3)	0.013(4)	0.10(2)
Q1 (S, Te)	18 h	0.77510(1)	0.22490(1)	0.110205(9)	0.01059(9)	0.017(2), 0.983	0.305(7), 0.695
Te2	6c	0	0	0.07441 (2)	0.0122(1)	1	1
S3	18f	0.31968(9)	0	0	0.0116(2)	1	1
S4	6c	0	0	0.36128(6)	0.0115(3)	1	1
S5	18 h	0.47630(5)	0.52370(5)	0.20644(3)	0.0112(2)	1	1

[a] Occupancies of $Ba_3Cu_{15.7(4)}S_{7.051(5)}Te_{3.949}$. [b] Occupancies of $Ba_3Cu_{15.1(1)}S_{7.92(2)}Te_{3.08}$. [c] Only present in $Ba_3Cu_{15.7(4)}S_{7.051(5)}Te_{3.949}$.

rhombohedral variant. For $y = 6$ and 7, respectively, the cubic variant was the primary phase with purity >95%, while larger values of y produced mixtures of both rhombohedral and cubic structures. Having $x < 0.5$, especially with large values of y, additionally produced the binary Cu_2Te, which was also noticed as a side product in the reaction with $x = 1$ and $y = 2$. During this study, the $Ba_3Cu_{17-x}S_{11.5-y}Te_y$ phase was treated as $Ba_3Cu_{17-x}S_{11-y}Te_y$, as the slightly different Ba/Q ratio (3:11.5 = 0.26 vs 3:11 = 0.27) was not a determining factor. Cu deficiencies are very common among Cu chalcogenides, likely because of the tendency to mixed valent Cu, so that x has to be >0 is not surprising.

A differential scanning calorimetry, DSC, measurement (using a NETZSCH STA 409PC Luxx[21,22]) performed under argon flow, revealed $Ba_3Cu_{16.5}S_4Te_7$ to be stable until approximately 900 K (Supporting Information).

Analysis. To prove the absence of heteroelements such as silicon stemming from the reaction container, two samples of nominal composition $Ba_3Cu_{17}S_8Te_3$ (rhombohedral variant) and $Ba_3Cu_{17}S_5Te_6$ (cubic variant) were analyzed via energy dispersive analysis of X-rays using an electron microscope (LEO 1530) with an additional EDX device (EDAX Pegasus 1200). The scans were performed with an acceleration voltage of 25 kV under high dynamic vacuum. No heteroelements were detected during the examination. The obtained Ba/Cu/S/Te ratios were reasonable with respect to the accuracy of the technique, yielding 9:57:29:6 atomic-%, as averaged over six crystals, compared to the nominal 9.7:54.8:25.8:9.7 in case of $Ba_3Cu_{17}S_8Te_3$, and 10:54:18:18 averaged over four crystals, compared to the nominal 9.7:54.8:16.1:19.4 in case of $Ba_3Cu_{17}S_5Te_6$.

Structure Determination. X-ray single crystal structure studies were performed on black block-like single crystals. A Bruker Smart APEX CCD diffractometer with graphite-monochromatized Mo−Kα radiation was used for the data collections, performed by scans of 0.3° in ω in two groups of 600 frames (each with an exposure time of 60 s) at $\phi = 0°$ and 90°. The data were corrected for Lorentz and polarization effects. Absorption corrections were based on fitting a function to the empirical transmission surface as sampled by multiple equivalent measurements using SADABS incorporated into the APEX II package.[23]

The structure solution and refinements were carried out with the SHELXTL program package.[24] The lattice parameters indicated either rhombohedral or cubic symmetry, depending on the S/Te ratio. Using a higher S than Te amount yields rhombohedral symmetry, to which no additional systematic absences were identified, leaving $R\bar{3}m$ as the space group of highest symmetry, as in $Ba_3Cu_{17-x}(Se,Te)_{11}$.[20] Thus, that model was used as a starting point for the refinements. As in case of the selenide-telluride before, the occupancies of all Cu sites were refined, yielding occupancies between 0.10(2) and 0.96(1). Similarly, all chalcogen sites (Q) were refined as being mixed albeit fully occupied by S and Te, allowing the S/Te ratio to vary freely. Of the five Q sites, one was occupied solely by Te (i.e., within its standard deviation of 2%), denoted

dx.doi.org/10.1021/ic200984q |Inorg. Chem. 2011, 50, 7831–7837

Te2, three by S (S3, S4, and S5), and one (Q1) was clearly mixed occupied (30.5(7)% S, 69.5% Te). In the final refinement, Te2 was fixed as a Te site and S3, S4, and S5 as S sites. This refinement yielded the formula of $Ba_3Cu_{15.1(1)}S_{7.92(2)}Te_{3.08}$.

When choosing a higher Te than S content, face-centered cubic symmetry was observed, without any (additional) systematic absences. Thus, the space group of highest symmetry is $Fm\bar{3}m$. The direct methods were used, which yielded eight atomic positions, to which one Ba, three Cu, one S, two mixed (S:Te) Q sites, and one Te sites were assigned based on interatomic distances and relative heights. On the basis of their displacement parameters, the Cu sites were treated as deficient, which gave refined occupancies between 50.0(8)% and 98.5(6)%. Refining the occupancies of Te2 and S3 did not show any significant deviations from full occupancy, and the presence of Te on the Q1 site may not be significant either. The formula was refined to be $Ba_3Cu_{16.0(1)}S_{4.45(4)}Te_{7.05}$. Standardization of the atomic positions was carried out with the TIDY program included in the PLATON package.[25]

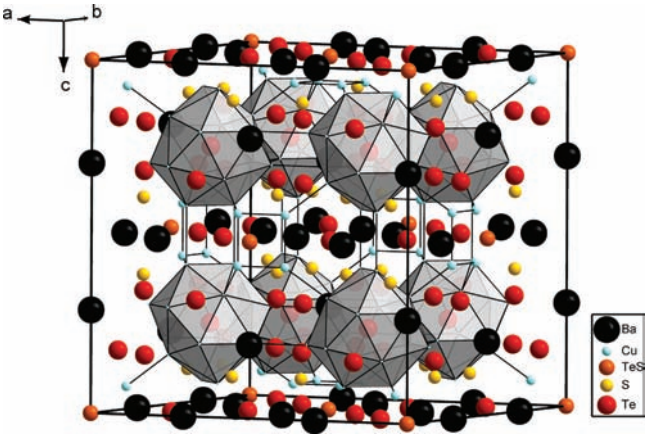

Figure 1. Unit cell of $Ba_3Cu_{17-x}(S,Te)_{11.5}$. The icosioctahedra are emphasized.

To prove the existence of a phase range and investigate its impact on the Q site occupancies, an additional crystal from each of the two structure types was analyzed. Their nominal compositions were $Ba_3Cu_{16}S_6Te_5$ (rhombohedral) and $Ba_3Cu_{17}S_5Te_6$ (cubic). In the first case, the formula was refined to $Ba_3Cu_{15.7(4)}S_{7.051(5)}Te_{3.949}$, with the second case refined to $Ba_3Cu_{15.6(2)}S_{5.33(4)}Te_{6.17}$, now with a significant amount of 14.2(5)% S on Q1. No evidence for ordering was found in either case. The crystallographic data are summarized in Table 1, and the atomic parameters including the occupancy factors in Table 2 (rhombohedral) and 3 (cubic).

Calculation of the Electronic Structure. We utilized the LMTO (linear muffin tin orbitals) method with the atomic spheres approximation, ASA, for the electronic structure calculations.[26,27] Therein, density functional theory is applied with the local density approximation, LDA, to treat correlation effects.[28] The following wave functions were used: for Ba 6s, 6p (downfolded[29]), 5d and 4f; for Cu 4s, 4p, and 3d, for S 3s, 3p, and 3d (downfolded) and for Te 5s, 5p, and 5d and 4f (the latter two downfolded). The eigenvalue problems were solved on the basis of 512 and 1000 irreproducible *k* points spread evenly in all

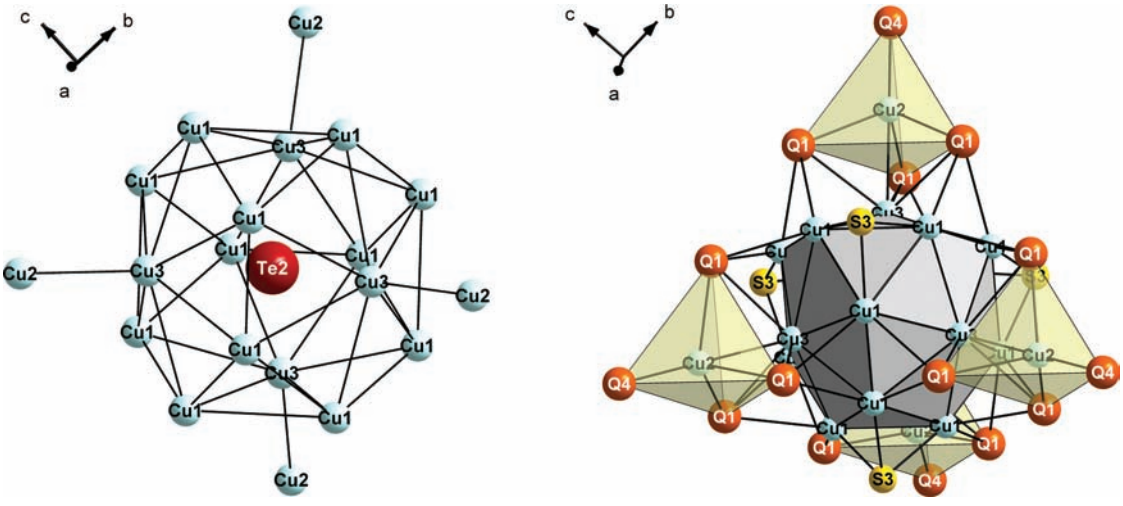

Figure 2. Cu_{16} icosioctahedron with four interconnecting Cu2−Cu3 bonds (left) and its extension with surrounding Q atoms (right).

Table 3. Atomic Coordinates and Equivalent Isotropic Displacement Parameters of $Ba_3Cu_{16.0(1)}S_{4.45(4)}Te_{7.05}$, and Occupancy Factors of $Ba_3Cu_{16.0(1)}S_{4.45(4)}Te_{7.05}$ and $Ba_3Cu_{15.6(2)}S_{5.33(4)}Te_{6.17}$

atom	site	*x*	*y*	*z*	U_{eq}/Å^2	occ.[a]	occ.[b]
Ba	24e	0.29213(5)	0	0	0.0134(2)	1	1
Cu1	96k	0.19950(4)	0.19950(4)	0.41664(8)	0.0327(4)	0.985(6)	0.923(7)
Cu2	32f	0.0745(1)	0.0745(1)	0.0745(1)	0.026(1)	0.500(8)	0.58(1)
Cu3	32f	0.1630(1)	0.1630(1)	0.1630(1)	0.026(1)	0.556(9)	0.55(1)
Q1 (S, Te)	48h	0	0.16969(3)	0.16969(3)	0.0140(2)	0.007(5), 0.993	0.142(5), 0.858
Te2	8c	1/4	1/4	1/4	0.0268(5)	1	1
S3	32f	0.3906(1)	0.3906(1)	0.3906(1)	0.0115(5)	1	1
Q4 (S, Te)	4a	0	0	0	0.038(3)	0.80(1), 0.20	0.95(2), 0.05

[a] Occupancies of $Ba_3Cu_{16.0(1)}S_{4.45(4)}Te_{7.05}$. [b] Occupancies of $Ba_3Cu_{15.6(2)}S_{5.33(4)}Te_{6.17}$.

dx.doi.org/10.1021/ic200984q |*Inorg. Chem.* 2011, 50, 7831–7837

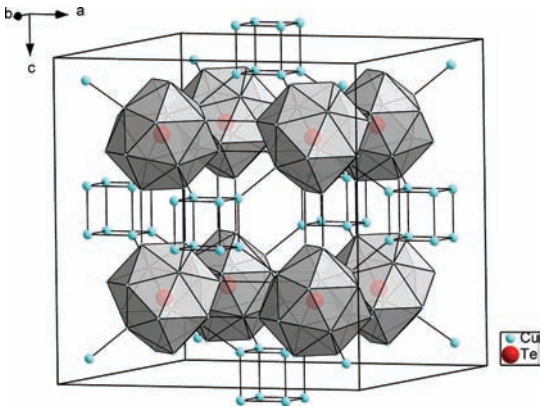

Figure 3. Three-dimensional network of Cu atoms with central Te2 atoms centering the icosioctahedra.

directions for cubic and rhombohedral structures, respectively, chosen with an improved tetrahedron method.[30]

The structural parameters were taken from the refinements on $Ba_3Cu_{15.1}S_{7.92}Te_{3.08}$ and $Ba_3Cu_{16.0}S_{4.45}Te_{7.05}$, respectively. These two structures were selected because the rhombohedral one had no split sites and the *Q*1 site of the cubic one was almost exclusively occupied by Te atoms; thus modeling *Q*1 as Te was most realistic. The sulfur-rich model was calculated with full Cu sites except for the removal of one of each Cu2 and Cu4 positions, while the 2/3 of *Q*1 sites were treated as Te and 1/3 as S, in accord with the experimental S occupancy of 0.31. As a result, this model has the formula $Ba_3Cu_{16}S_8Te_3$ in space group *Cm*. The second, originally cubic, model was calculated in *I*4*mm* by removing half of the eight Cu2 and half of eight Cu3 positions, where *Q*1 was treated as Te and *Q*4 as S, to yield $Ba_3Cu_{16}S_{4.5}Te_7$.

Physical Property Measurements. Cold-pressed bars of the dimensions 6 × 1 × 1 mm of selected samples from rhombohedral and cubic settings were used for Seebeck coefficient (S) and electrical conductivity (σ) measurements. S and σ were simultaneously measured on a commercial ULVAC-RIKO ZEM-3 instrument from room temperature up to 750 K. The specific electrical conductivity (σ) is determined via the four-point-method, and the Seebeck coefficient via $S = \Delta V/\Delta T$; thermocouple probe separation was approximately 3 mm for these studies. The achieved density was around 85% of the theoretical maximum determined via the single crystal structure study. The resistances (R) were calculated from the voltage drops using Ohm's law, that is, $R = \Delta V/I$, with I = current. $\sigma(T)$ was calculated after measuring the lengths between the contacts, L, according to $\sigma = L/(AR)$, with the area A = 1 mm × 1 mm.

RESULTS AND DISCUSSION

Crystal Structure. The rhombohedral selenide-telluride was described in 2009.[20] Like the selenide-telluride, the rhombohedral sulfide-telluride features interconnected Cu_{26} clusters, which are composed of two stacked hexagonal antiprisms capped on both terminal hexagonal faces. The unit cell is composed of a series of corner-, edge-, and face-sharing CuQ_4 tetrahedra. Four of the six Cu sites are essentially fully occupied, with occupancies between 92% and 98%, while the occupancies of Cu5 and Cu6 can range anywhere between 50% and 80% or 10% and 60%, respectively. In the case of tellurium-richer $Ba_3Cu_{15.7(4)}S_{7.051(5)}Te_{3.949}$, however, Cu2 had to be refined as a split site, while the Cu6 site was virtually unoccupied (refined to be 1.3%), in contrast to 10% in case of $Ba_3Cu_{15.1(1)}S_{7.92(2)}Te_{3.08}$. This can be rationalized as Cu atoms being forced into different sites to compensate for the nearly Te-exclusive *Q*1 site (Table 2), typically between 46% and 74% Te with the selenides, as Cu6 is surrounded by three *Q*1 atoms. Besides *Q*1, all other *Q* sites (2 through 5) were found to be exclusively occupied by either S or Te atoms.

The crystal structure of the cubic variant, realized in $Ba_3Cu_{16.0(1)}S_{4.45(4)}Te_{7.05}$ and $Ba_3Cu_{15.6(2)}S_{5.33(4)}Te_{6.17}$, is also composed of a three-dimensional network of corner-, edge-, and face-sharing CuQ_4 tetrahedra. For example, the $Cu2Q_4$ and $Cu3Q_4$ tetrahedra share a common face formed by three Te1 atoms. The Ba cations are centered in square antiprisms composed of two $Q1_4$ faces, and the square antiprisms are interconnected via common edges.

Table 4. Selected Interatomic Distances [Å] of $Ba_3Cu_{17-x}(S,Te)_{11}$ (top) and $Ba_3Cu_{17-x}(S,Te)_{11.5}$ (bottom)

		distance range			distance range
		$Ba_3Cu_{17-x}(S,Te)_{11}$			
Ba	Q1	2× 3.5662(8)−3.6047(4)	Cu1	Cu1 3×	2.458(3)−2.894(4)
	S3	2× 3.268(2)−3.3004(7)		Cu3 1×	2.811(2)−2.8171(7)
	S4	1× 3.2829(9)−3.298(3)		Cu4 1×	2.746(3)−2.7645(7)
	S5	3× 3.1169(7)−3.322(1)		Cu5 1×	2.8224(6)−2.830(3)
				Q1 2×	2.666(2)−2.7605(5)
Cu2	Cu2B	3× '0.40(2)', 3.06(3)		Te2 1×	3.126(2)−3.154(2)
	Cu3	1× 2.70(1)−2.800(4)		S5 1×	2.213(3)−2.2365(9)
	Cu4	1× 2.63(1)−2.663(4)			
	Cu6	1× 2.42(4)−2.90(4)	Cu3	Cu1 2×	2.811(2)−2.8171(7)
	Q1	1× 2.585(3)−2.669(8)		Cu2B 2×	2.92(2)
	S3	2× 2.565(8)−2.613(2)		Cu4 3×	2.712(3)−2.7764(5)
	S4	1× 2.228(4)−2.29(1)		Te2 1×	3.039(2)−3.0556(7)
				S3 2×	2.395(2)−2.4116(7)
Cu2B	Cu2	1× 3.06(2)		S5 1×	2.306(4)−2.317(1)
	Cu2B	2× '0.68(4)', 2.71(4)			
	Cu6	1× 2.24(5)	Cu4	Cu1 2×	2.746(3)−2.7645(7)
	Q1	1× 2.645(8)		Cu2 1×	2.63(1)−2.663(4)
	S3	1× 2.48(2)		Cu2B 2×	2.81(2)
	S4	1× 2.19(1)		Cu3 3××	2.712(3)−2.7764(5)
				Q1 1×	2.812(3)−2.8323(7)
Cu5	Cu1	6× 2.8224(6)−2.830(3)		Te2 1×	2.615(2)−2.6167(7)
	Cu6	1× 1.84(5)−2.81(7)		S3 2×	2.429(3)−2.4439(8)
	Q1	3× 2.701(3)−2.7520(7)			
	Te2	1× 2.523(6)−2.552(1)	Cu6	Cu2 3×	2.42(4)−2.90(4)
				Cu2B 5×	2.24(5)
				Cu5 1×	1.84(5)−2.81(7)
				Q1 3×	2.268(7)−2.57(4)
				S4 1×	3.43(5)−2.60(8)
		$Ba_3Cu_{17-x}(S,Te)_{11.5}$			
Ba	Q1	4× 3.5932(6)−3.6067(5)	Cu1	Cu1 4×	2.461(2)−2.874(3)
	S3	4× 3.161(1)−3.167(1)		Cu3 2×	2.810(1)−2.819(2)
				Q1 2×	2.714(1)−2.7224(9)
Cu2	Cu2	3× 2.543(5)−2.567(4)		S3 1×	2.233(2)−2.242(2)
	Cu3	1× 2.640(6)−2.642(5)		Te2 1×	3.125(1)−3.134(2)
	Q1	3× 2.652(2)−2.653(2)			
	Q4	1× 2.202(4)−2.223(4)	Cu3	Cu1 6×	2.810(2)−2.819(2)
				Q1 3×	2.801(2)−2.814(2)
				Te2 1×	2.598(3)−2.610(4)

dx.doi.org/10.1021/ic200984q |*Inorg. Chem.* 2011, 50, 7831–7837

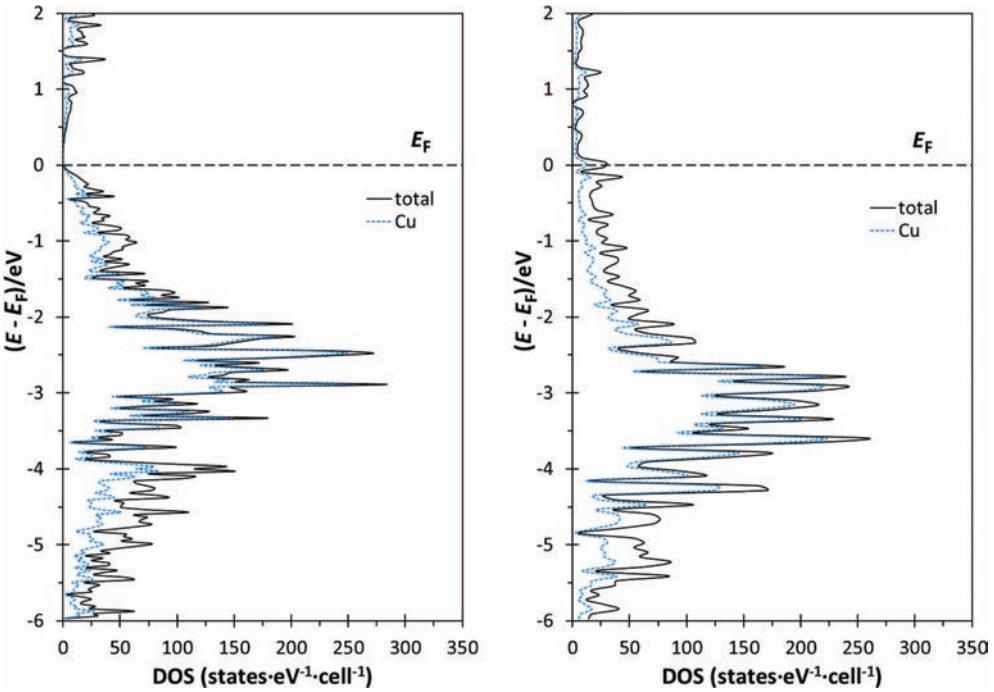

Figure 4. Density of states of $Ba_3Cu_{16}S_8Te_3$ in *Cm* (left) and of $Ba_3Cu_{16}S_{4.5}Te_7$ in *I4mm* (right).

Since no short *Q*−*Q* contacts occur in this structure, the oxidation states are therefore assigned to Ba^{2+}, Cu^{+}, and Q^{2-}. Thus, the chalcogenides with $x = 0$, that is, $Ba_3Cu_{17}(S,Te)_{11.5}$, are electron precise. The Cu_{16} clusters are regular icosioctahedra (emphasized in Figure 1), as sometimes found in intermetallics such as $Na_{35}Cd_{24}Ga_{56}$[31] and $Mg_{35}Cu_{24}Ga_{53}$.[32] To our knowledge, this is the first time that such an icosioctahedron is centered by a chalcogen atom.

The Cu_{16} icosioctahedron is centered by a Te2 atom, and its 28 triangular faces are formed by 12 Cu1 atoms and 4 Cu3 atoms, subsequently of point symmetry *T* (left part of Figure 2). While Cu1 is almost fully occupied (refined values were 92%−99%), Cu3 is roughly half occupied, so that the averaged coordination number of Te2 is about $12 \times 1 + 4 \times 2 = 14$. Each Cu3 atom is bonded to one Cu2 atom, which in turn forms $Cu2_8$ cubes located between the icosioctahedra. S3 atoms are bonded to three Cu1 atoms on each of the four triangular icosioctahedron faces that are not coordinated to Cu3 (right part of Figure 2). The intracluster distances of 2.46 Å−2.81 Å (Table 4) are typical Cu−Cu bonds, as found in several other Cu-chalcogenides,[33] including $Ba_3Cu_{14-x}Te_{12}$[8] and $Ba_3Cu_{17-x}(Se,Te)_{11}$,[20] noting that these formally closed-shell (d^{10}−d^{10}) interactions occur regularly in Cu chalcogenides, and their bonding character arises from mixing of the filled *d* states with the nominally empty, energetically higher lying *s* and *p* orbitals.[34−36]

As can be observed in Figure 3, the Cu atom network is three-dimensional, with the icosioctahedra being connected to 6 other icosioctahedra via 12 intercluster Cu1−Cu1 contacts of around 2.87 Å, of which Figure 3 shows only those connected in one unit cell; each icosioctahedron joins others in three neighboring unit cells along [100], [010], and [001]. Additionally, each icosioctahedron is bonded to four Cu2 atoms from each of the polyhedron's Cu3 sites. The Cu2 atoms form cubes centered by *Q*4 atoms with Cu2−Q4 bonds of 2.20 Å−2.22 Å, with Cu2−Cu2 distances along the edges of approximately 2.55 Å. With the occupancy of Cu2 between 50% and 58%, the averaged coordination number of *Q*4, dominated by S atoms, is about 8/2 = 4. Similarly, the Cu cubes of $BaCu_{5.9}STe_6$ were centered by S atoms, with Cu−S bonds of 2.33 Å and a Cu occupancy of 74%, resulting in an average coordination number of $8 \times 3/4 = 6$ for this S atom.[10] Because of the three-dimensional extension of the Cu−Cu contacts in combination with the Cu deficiencies of Cu2 and Cu3 (each on the order of 50%), Cu ion conductivity appears to be likely in $Ba_3Cu_{17-x}(Se,Te)_{11.5}$, as previously shown for $Ba_3Cu_{17-x}(Se,Te)_{11}$, though the anisotropic displacement parameters are not as large and distinctly anisotropic as found in the best Cu ion conductors including $Rb_4Cu_{16}I_7Cl_{13}$[37,38] and Cu_6PS_5Cl.[39]

While no mixed S:Te occupancies were identified in the sulfide-tellurides $Ba_2Cu_{6-x}STe_4$[10] and Zr_6STe_2,[40] each of the four crystals investigated here has at least one mixed S:Te site, with ratios of up to 30:70 and 80:20, respectively. Other examples for mixed S:Te occupancies, while rare, do exist, including $Ta_6S_{1+x}Te_{3-x}$[41] (with up to 4% S on Te sites and 7% Te on S sites) and $Ta_{15}Si_2S_xTe_{10-x}$[42] (with one pure S site and four mixed S:Te sites, albeit with very high standard deviations). It is most probable that, because of the large difference in atom sizes, the S and Te atoms do not occupy the same absolute position. This seems to be not resolvable from the X-ray data, but it is reflected in large displacement parameters of the sites involved, for example, *Q*4 and its neighboring Cu2 in case of $Ba_3Cu_{17-x}(S,Te)_{11.5}$. In this case, Te on *Q*4 is very likely to be surrounded by more deficient Cu2 cubes and to be placed off-center because of the short averaged Cu2−*Q*4 distance of 2.2 Å.

Electronic Structure. The density of states, DOS, of the electron precise model $Ba_3Cu_{16}S_8Te_3$ reveal a small band gap of the order of 0.12 eV at the Fermi level (left part of Figure 4). The area below the Fermi level, E_F, is predominated by Cu 3d

dx.doi.org/10.1021/ic200984q |*Inorg. Chem.* 2011, 50, 7831–7837

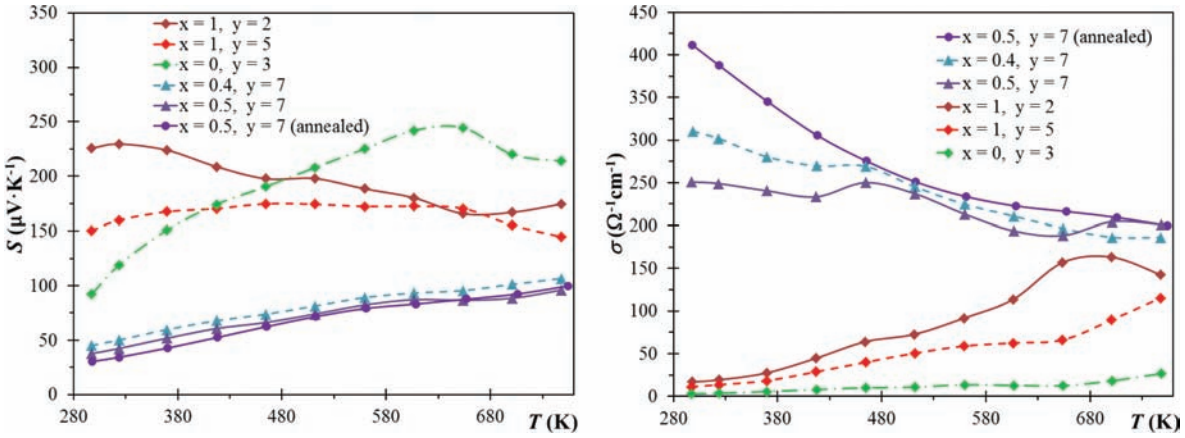

Figure 5. Seebeck coefficient (left) and electrical conductivity (right) of $Ba_3Cu_{17-x}S_{11-y}Te_y$ (diamonds) and $Ba_3Cu_{17-x}S_{11.5-y}Te_y$ (triangles/circles).

states with contributions from the S 3p and Te 5p states, and the conduction band consists of Ba s, Cu s, and Cu p states. The $Ba_3Cu_{16}S_{4.5}Te_7$ model (right part of Figure 4) possesses no band gap at the Fermi level, but has a very few states immediately above the Fermi level with some minima at approximately 0.5 and 0.8 eV; this metal-like DOS would suggest a small Seebeck coefficient, which can be verified in the following section. The energy levels below the Fermi level are again predominantly Cu 3d states and chalcogen p states.

Physical Properties. The rhombohedral sulfide-tellurides showed physical properties that were comparable to that of the previously studied selenide material published in 2009.[20] Measurements were performed on rhombohedral $Ba_3Cu_{16}S_6Te_5$, $Ba_3Cu_{17}S_8Te_3$ and $Ba_3Cu_{16}S_9Te_2$ (Figure 5). Seebeck coefficient values were mostly between $S = +150\ \mu V\ K^{-1}$ and $+250\ \mu V\ K^{-1}$ for the full range of the measurement. Electrical conductivity values were all below $\sigma = 20\ \Omega^{-1}\ cm^{-1}$ at room temperature and gently increased with the temperature, as is expected of a slightly doped semiconductor, reaching a maximum of $163\ \Omega^{-1}\ cm^{-1}$ at 700 K for $Ba_3Cu_{16}S_9Te_2$. The resulting highest power factor $P.F. = S^2\sigma$ at room temperature was 0.45 $\mu W\ cm^{-1}\ K^{-2}$ for $Ba_3Cu_{16}S_9Te_2$, which reached 2.38 $\mu W\ cm^{-1}\ K^{-2}$ at 700 K.

For the cubic materials of nominal composition "$Ba_3Cu_{16.5}S_4Te_7$" (measured directly after cold-pressing as well as after cold-pressing and sintering at 825 K) and "$Ba_3Cu_{16.6}S_4Te_7$", S, being almost unaffected by the annealing process, rose gradually from about $+40\ \mu V\ K^{-1}$ to $+100\ \mu V\ K^{-1}$. The electrical conductivity behaved like a metal or degenerate semiconductor, showing a gradually decreasing slope as temperature rises. The annealed sample exhibited, not surprisingly, the highest value at room temperature, namely $412\ \Omega^{-1}\ cm^{-1}$, while the cold-pressed samples showed comparable conductivity curves beginning around 465 K. The σ of the three cubic samples decreased to about $200\ \Omega^{-1}\ cm^{-1}$ at 750 K. The highest power factor at room temperature was 0.63 $\mu W\ cm^{-1}\ K^{-2}$ for cubic, annealed "$Ba_3Cu_{16.6}S_4Te_7$", which reached 2.12 $\mu W\ cm^{-1}\ K^{-2}$ at 750 K.

For comparison, the S values at room temperature of other barium copper chalcogenides were $+35\ \mu V\ K^{-1}$ for $Ba_3Cu_{13.88}Te_{12}$,[8] $+100\ \mu V\ K^{-1}$ for $BaCu_{5.7}Se_{0.6}Te_{6.4}$,[10] and $+120\ \mu V\ K^{-1}$ for $K_2BaCu_8Te_{10}$,[7] with σ(300 K) of these three materials being $190\ \Omega^{-1}\ cm^{-1}$, $40\ \Omega^{-1}\ cm^{-1}$, and $70\ \Omega^{-1}\ cm^{-1}$, respectively. Thus, the last three materials exhibited comparable power factors, ranging from $P.F. = 0.2\ \mu W\ cm^{-1}\ K^{-2}$ to $1.0\ \mu W\ cm^{-1}\ K^{-2}$ at 300 K.

CONCLUSIONS

Two structure types were discovered for the Ba−Cu-(S,Te) system, which are dependent not only on the crucial mixing of both S and Te atoms but on the S/Te ratio as well. The rhombohedral variant is found when [S] > [Te] and shows mixing on the Q1 site, with the Cu5 and Cu6 atoms displaying large deficiencies. The Cu cages are based on Cu_{26} clusters, topologically equivalent to the previously published $Ba_3Cu_{17-x}(Se,Te)_{11}$. Upon introducing [Te] > [S], a new, cubic structure type is found: $Ba_3Cu_{17-x}(S,Te)_{11.5}$, also with mixed S:Te occupancies. Two of three Cu sites have between 50% and 58% occupancies and form regular Cu_{16} icosioctahedra of point symmetry T, eight of which are found in one unit cell, all interconnected via additional Cu_8 cubes to an infinite Cu atom network. Phase width studies indicate that both structures require a Cu-deficiency, a common observation in many Cu chalcogenides, and like in case of the previously reported rhombohedral selenide-telluride, at least a ~1:4 mixture of the two different chalcogen atoms is required for the formation of these structures. The cubic structure will form as soon as the Te content is higher than the S content, as became evident when comparing the structures of nominal compositions $Ba_3Cu_{16}S_5Te_6$ and $Ba_3Cu_{16}S_6Te_5$.

The electronic structure calculations suggest that $Ba_3Cu_{17-x}(S,Te)_{11}$ would be an intrinsic p-type semiconductor when $x = 1$, which is in agreement with the measurement of three stoichiometric variations thereof. The highest power factor was found to be 2.38 $\mu W\ cm^{-1}\ K^{-2}$ at 700 K, but like in case of its Se-counterpart, high Cu ion mobility makes this material a poor choice for thermoelectric materials. The calculations for $Ba_3Cu_{17-x}(S,Te)_{11.5}$ revealed a significant albeit small number of states around the Fermi level, which concurs well with its smaller Seebeck coefficient and larger electrical conductivity. The highest power factor of this series, 2.12 $\mu W\ cm^{-1}\ K^{-2}$ at 750 K, is very comparable to the maximum measured for $Ba_3Cu_{17-x}(S,Te)_{11}$. Here as well, the structure refinements suggest the possibility of a high Cu mobility that makes it unappealing from a thermoelectric perspective.

ASSOCIATED CONTENT

Supporting Information. Four crystallographic information files (CIFs), and one DSC/TG curve for $Ba_3Cu_{16.5}S_4Te_7$.

This material is available free of charge via the Internet at http://pubs.acs.org.

AUTHOR INFORMATION

Corresponding Author
*E-mail: kleinke@uwaterloo.ca.

ACKNOWLEDGMENT

Financial support from NSERC, CFI, OIT (Ontario Distinguished Researcher Award for H.K.), and the Canada Research Chair program (CRC for H.K.) is appreciated.

REFERENCES

(1) Lowhorn, N. D.; Tritt, T. M.; Abbott, E. E.; Kolis, J. W. *Appl. Phys. Lett.* **2006**, *88*, 022101/1–022101/3.
(2) Nilges, T.; Lange, S.; Bawohl, M.; Deckwart, J. M.; Jansen, M.; Wiemhöfer, H.-D.; Decourt, R.; Chevalier, B.; Vannahme, J.; Eckert, H.; Weihrich, R. *Nat. Mater.* **2009**, *8*, 101–108.
(3) Tritt, T. M. *Science* **1996**, *272*, 1276–1277.
(4) DiSalvo, F. J. *Science* **1999**, *285*, 703–706.
(5) Rowe, D. M. *Thermoelectrics Handbook: Macro to Nano*; CRC Press, Taylor & Francis Group: Boca Raton, FL, 2006.
(6) Wang, Y. C.; DiSalvo, F. J. *J. Solid State Chem.* **2001**, *156*, 44–50.
(7) Patschke, R.; Zhang, X.; Singh, D.; Schindler, J.; Kannewurf, C. R.; Lowhorn, N.; Tritt, T.; Nolas, G. S.; Kanatzidis, M. G. *Chem. Mater.* **2001**, *13*, 613–621.
(8) Assoud, A.; Thomas, S.; Sutherland, B.; Zhang, H.; Tritt, T. M.; Kleinke, H. *Chem. Mater.* **2006**, *18*, 3866–3872.
(9) Mayasree, O.; Sankar, C. R.; Assoud, A.; Kleinke, H. *Inorg. Chem.* **2011**, *50*, 4580–4585.
(10) Mayasree, O.; Sankar, C. R.; Cui, Y.; Assoud, A.; Kleinke, H. *Eur. J. Inorg. Chem.* **2011**, in press.
(11) Mayasree, O.; Cui, Y.; Assoud, A.; Kleinke, H. *Inorg. Chem.* **2010**, *49*, 6518–6524.
(12) Yao, X.; Marking, G.; Franzen, H. F. *Ber. Bunsenges.* **1992**, *96*, 1552–1557.
(13) Köckerling, M.; Franzen, H. F. *Croat. Chem. Acta* **1995**, *68*, 709–719.
(14) Kleinke, H. *Trends Inorg. Chem.* **2001**, *7*, 135–149.
(15) Kleinke, H. *J. Alloys Compd.* **2002**, *336*, 132–137.
(16) Yao, X.; Franzen, H. F. *J. Am. Chem. Soc.* **1991**, *113*, 1426–1427.
(17) Yao, X.; Miller, G. J.; Franzen, H. F. *J. Alloys Compd.* **1992**, *183*, 7–17.
(18) Yao, X.; Franzen, H. F. *J. Solid State Chem.* **1990**, *86*, 88–93.
(19) Yao, X.; Franzen, H. F. *Z. Anorg. Allg. Chem.* **1991**, *598*−*599*, 353–362.
(20) Kuropatwa, B.; Cui, Y.; Assoud, A.; Kleinke, H. *Chem. Mater.* **2009**, *21*, 88–93.
(21) Assoud, A.; Soheilnia, N.; Kleinke, H. *Chem. Mater.* **2005**, *17*, 2255–2261.
(22) Lee, C.-S.; Kleinke, K. M.; Kleinke, H. *Solid State Sci.* **2005**, *7*, 1049–1054.
(23) *M86-Exx078 APEX2 User Manual*; Bruker AXS Inc.: Madison, WI, 2006.
(24) Sheldrick, G. M. *Acta Crystallogr.* **2008**, *64*, 112–122.
(25) Spek, A. L. *J. Appl. Crystallogr.* **2003**, *36*, 7–13.
(26) Andersen, O. K. *Phys. Rev. B* **1975**, *12*, 3060–3083.
(27) Skriver, H. L. *The LMTO Method*; Springer: Berlin, Germany, 1984.
(28) Hedin, L.; Lundqvist, B. I. *J. Phys. C* **1971**, *4*, 2064–2083.
(29) Lambrecht, W. R. L.; Andersen, O. K. *Phys. Rev. B* **1986**, *34*, 2439–2449.
(30) Blöchl, P. E.; Jepsen, O.; Andersen, O. K. *Phys. Rev. B* **1994**, *49*, 16223–16233.
(31) Tillard-Charbonnel, M.; Belin, C. *Mater. Res. Bull.* **1992**, *27*, 1277–86.
(32) Lin, Q.; Corbett, J. D. *Inorg. Chem.* **2005**, *44*, 512–518.
(33) Jansen, M. *Angew. Chem., Int. Ed. Engl.* **1987**, *26*, 1098–1110.
(34) Mehrotra, P. K.; Hoffmann, R. *Inorg. Chem.* **1978**, *17*, 2187–2189.
(35) Merz, K. M., Jr.; Hoffmann, R. *Inorg. Chem.* **1988**, *27*, 2120–2127.
(36) Pyykkö, P. *Chem. Rev.* **1997**, *97*, 597–636.
(37) Owens, B. B. *J. Power Sources* **2000**, *90*, 2–8.
(38) Kanno, R.; Ohno, K.; Kawamoto, Y.; Takeda, Y.; Yamamoto, O.; Kamiyama, T.; Asano, H.; Izumi, F.; Kondo, S. *J. Solid State Chem.* **1993**, *102*, 79–92.
(39) Gagor, A.; Pietraszko, A.; Kaynts, D. *J. Solid State Chem.* **2008**, *181*, 777–782.
(40) Örlygsson, G.; Conrad, M.; Harbrecht, B. *Z. Anorg. Allg. Chem.* **2001**, *627*, 1017–1022.
(41) Debus, S.; Harbrecht, B. *Z. Anorg. Allg. Chem.* **2000**, *626*, 173–179.
(42) Debus, S.; Harbrecht, B. *Z. Anorg. Allg. Chem.* **2001**, *627*, 431–438.